

Stoichiometric Network Analysis of the Bray-Liebhaufsky Reaction

Akshat Goyal (2018101075), Kanish Anand (2018101025)
IIIT Hyderabad

Abstract

The stoichiometric network analysis (SNA) is applied to a simplified model of the complex oscillating Bray-Liebhaufsky reaction under batch conditions. This powerful method for the analysis of steady-states stability is also used to transform the classical differential equations into dimensionless equations. This simplifies greatly the study of the slow manifold and shows which parameters are essential for controlling its shape and consequently have an important influence on the trajectories. We have also added time course simulations and phase portrait plots.

1. Introduction

A chemical oscillator is a complex mixture of reacting chemical compounds in which the concentration of one or more components exhibits periodic changes. They are a class of reactions that serve as an example of non-equilibrium thermodynamics with far-from-equilibrium behavior. The reactions are theoretically important in that they show that chemical reactions do not have to be dominated by equilibrium thermodynamic behavior. In cases where one of the reagents has a visible color, periodic color changes can be observed. Examples of oscillating reactions are the Belousov-Zhabotinsky reaction (BZ), the Briggs-Rauscher reaction, and the Bray-Liebhaufsky reaction.

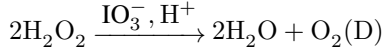
Chemical systems cannot oscillate about a position of final equilibrium because such an oscillation would violate the second law of thermodynamics. For a thermodynamic system which is not at equilibrium, this law requires that the system approach equilibrium and not recede from it. For a closed system at constant temperature and pressure, the thermodynamic requirement is that the Gibbs free energy must decrease continuously and not oscillate. However it is possible that the concentrations of some reaction intermediates oscillate, and also that the rate of formation of products oscillates. Theoretical models of oscillating reactions have been studied by chemists, physicists, and mathematicians. In an oscillating system the energy-releasing reaction can follow at least two different pathways, and the reaction pe-

riodically switches from one pathway to another. One of these pathways produces a specific intermediate, while another pathway consumes it. The concentration of this intermediate triggers the switching of pathways. When the concentration of the intermediate is low, the reaction follows the producing pathway, leading then to a relatively high concentration of intermediate. When the concentration of the intermediate is high, the reaction switches to the consuming pathway. Different theoretical models for this type of reaction have been created, including the Lotka-Volterra model, the Brusselator and the Oregonator. The latter was designed to simulate the Belousov-Zhabotinsky reaction.

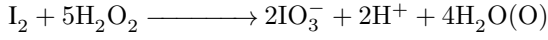
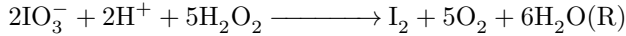
Continuous dynamical systems that involve differential equations mostly contain parameters. It can happen that a slight variation in a parameter can have significant impact on the solution. The main questions of interest are: How to continue equilibria and periodic orbits of dynamical systems with respect to a parameter? How to compute stability boundaries of equilibria and limit cycles in the parameter space? How to predict qualitative changes in system's behavior (bifurcations) occurring at these equilibrium points? We will analyse the specific bifurcation called **Hopf bifurcation** which refers to the development of periodic orbits from stable equilibrium point, as a bifurcation parameter crosses a critical value. Since the theory of bifurcation from equilibria based on center manifold reduction and Poincaré-Normal forms, the direction of bifurcations for the mathematical models will also be explained using this theory. In general, in a dynamical system, a parameter is allowed to vary, then the differential system may change. An equilibrium can become unstable and a periodic solution may appear or a new stable equilibrium may appear making the previous equilibrium unstable. The value of parameter at which these changes occur is known as *bifurcation value* and the parameter that is varied is known as the *bifurcation parameter*.

2. Bray-Liebhaufsky Reaction

The Bray-Liebhaufsky reaction is the decomposition of hydrogen peroxide in the presence of iodate and hydrogen ions, which can be presented by the following simple process:



This decomposition is the result of two complex reactions in which hydrogen peroxide acts as either a reducing (R) or an oxidizing (O) agent. However, multiple intermediary species such as I_2 , I^- , HIO , HIO_2 and I_2O are involved in the complex reaction network underlying this schematic representation. Therefore, beside simple oscillations in concentrations of these intermediary species, complex oscillations and chaos are also obtained in this reaction system.



The sum of reactions R and O gives reaction D. When the rates of these two reactions are equal, the decomposition of hydrogen peroxide is monotonous. However, under some conditions discussed in this paper, the reactions R and O dominate alternately, resulting in a cascading consumption of hydrogen peroxide and an oscillatory evolution of the intermediates.

2.1. The Extreme Currents

The fundamental idea of the SNA is to express the rates of reactions using new sets of variables and parameters. The variables are the ratios between the actual concentrations and their values at a steady-state and the parameters are some rates at this steady-state. Thus we need to define the steady-state chosen as reference. Here it is the smooth decomposition of hydrogen peroxide (D) called “the disproportionation steadystate”. The decomposition of hydrogen peroxide under batch conditions is slow at the considered time scale, and therefore we can assume that the concentration of hydrogen peroxide, as well as iodate and acid concentrations, is constant during the time of interest. These compounds are called external.

TABLE 1: Model of the Bray–Liebhafsky Reaction

reactions	no.
$\text{IO}_3^- + \text{I}^- + 2\text{H}^+ \rightleftharpoons \text{IOH} + \text{IO}_2\text{H}$	(R1), (R-1)
$\text{IO}_2\text{H} + \text{I}^- + \text{H}^+ \rightarrow \text{I}_2\text{O} + \text{H}_2\text{O}$	(R2)
$\text{I}_2\text{O} + \text{H}_2\text{O} \rightleftharpoons 2\text{IOH}$	(R3), (R-3)
$\text{IOH} + \text{I}^- + \text{H}^+ \rightleftharpoons \text{I}_2 + \text{H}_2\text{O}$	(R4), (R-4)
$\text{IOH} + \text{H}_2\text{O}_2 \rightarrow \text{I}^- + \text{H}^+ + \text{O}_2 + \text{H}_2\text{O}$	(R5)
$\text{I}_2\text{O} + \text{H}_2\text{O}_2 \rightarrow \text{IOH} + \text{IO}_2\text{H}$	(R6)
$\text{IO}_3^- + \text{H}^+ + \text{H}_2\text{O}_2 \rightarrow \text{IO}_2\text{H} + \text{O}_2 + \text{H}_2\text{O}$	(R8)

a

Denoting by \mathbf{S} the matrix of the stoichiometric coefficients in the model and by s its rank, all the extreme currents are obtained looking for all nontrivial solutions with

no negative component of the s independent equations $\mathbf{S} \mathbf{E}_i = 0$. The \mathbf{E}_i vectors are determined only up to a positive factor that is usually chosen to get round numbers. The set of extreme currents for a given factor is unique and is represented by the \mathbf{E} matrix where each row comes from one step of the model. For the model in Table 1, we have the following matrices:

$$\mathbf{S} = \begin{array}{c|cccccccccc|l} & (\text{R1}) & (\text{R-1}) & (\text{R2}) & (\text{R3}) & (\text{R-3}) & (\text{R4}) & (\text{R-4}) & (\text{R5}) & (\text{R6}) & (\text{R8}) & \\ \hline & 0 & 0 & 0 & 0 & 0 & 1 & -1 & 0 & 0 & 0 & \text{I}_2 \\ & -1 & 1 & -1 & 0 & 0 & -1 & 1 & 1 & 0 & 0 & \text{I}^- \\ & 1 & -1 & 0 & 2 & -2 & -1 & 1 & -1 & 1 & 0 & \text{IOH} \\ & 1 & -1 & -1 & 0 & 0 & 0 & 0 & 0 & 1 & 1 & \text{IO}_2\text{H} \\ & 0 & 0 & 1 & -1 & 1 & 0 & 0 & 0 & -1 & 0 & \text{I}_2\text{O} \end{array}$$

$$\mathbf{E} = \begin{array}{ccccc|l} & \mathbf{E}_1 & \mathbf{E}_2 & \mathbf{E}_3 & \mathbf{E}_4 & \mathbf{E}_5 & \\ \hline & 1 & 0 & 0 & 0 & 0 & (\text{R1}) \\ & 1 & 0 & 0 & 0 & 1 & (\text{R-1}) \\ & 0 & 0 & 0 & 1 & 1 & (\text{R2}) \\ & 0 & 1 & 0 & 0 & 0 & (\text{R3}) \\ & 0 & 1 & 0 & 0 & 0 & (\text{R-3}) \\ & 0 & 0 & 1 & 0 & 0 & (\text{R4}) \\ & 0 & 0 & 1 & 0 & 0 & (\text{R-4}) \\ & 0 & 0 & 0 & 1 & 0 & (\text{R5}) \\ & 0 & 0 & 0 & 1 & 1 & (\text{R6}) \\ & 0 & 0 & 0 & 0 & 1 & (\text{R8}) \end{array}$$

In the SNA, the rates at the steady state r_{ss} are expressed as linear combinations of the columns of \mathbf{E} , $\mathbf{r}_{ss} = \mathbf{E} \mathbf{j}$.

$$\begin{aligned} (r_{+1})_{ss} &= k_{+1}[\text{I}^-]_{ss} = j_1 \\ (r_{-1})_{ss} &= k_{-1}[\text{IOH}]_{ss}[\text{IO}_2\text{H}]_{ss} = j_1 + j_5 \\ (r_2)_{ss} &= k_2[\text{IO}_2\text{H}]_{ss}[\text{I}^-]_{ss} = j_4 + j_5 \\ (r_{+3})_{ss} &= k_{+3}[\text{I}_2\text{O}]_{ss} = j_2 \\ (r_{-3})_{ss} &= k_{-3}[\text{IOH}]_{ss}^2 = j_2 \\ (r_{+4})_{ss} &= k_{+4}[\text{IOH}]_{ss}[\text{I}^-]_{ss} = j_3 \\ (r_{-4})_{ss} &= k_{-4}[\text{I}_2]_{ss} = j_3 \\ (r_5)_{ss} &= k_5[\text{IOH}]_{ss} = j_4 \\ (r_6)_{ss} &= k_6[\text{I}_2\text{O}]_{ss} = j_4 + j_5 \\ (r_8)_{ss} &= k_8 = j_5 \end{aligned}$$

2.2. Rate Equations and Stability Analysis

The stability of a steady state can be analyzed by linearization of the stoichiometric network general equation of motion about this steady state. The SNA theory simplifies greatly this analysis using the j'_i s as parameters and the ratios between the actual concentrations and their values at the steady-state as variables. Thus, we define $x_1 = [\text{I}_2]/[\text{I}_2]_{ss}$, $x_2 = [\text{I}^-]/[\text{I}^-]_{ss}$, $x_3 = [\text{IOH}]/[\text{IOH}]_{ss}$, $x_4 = [\text{IO}_2\text{H}]/[\text{IO}_2\text{H}]_{ss}$, $x_5 = [\text{I}_2\text{O}]/[\text{I}_2\text{O}]_{ss}$, write the rate equations as functions of these variables, for example $r_{+1} = k_{+1}[\text{I}^-]_{ss} x_2 = j_1 x_2$, and obtain the equations of motion in the following form.

$$\begin{aligned}
[I_2]_{ss} \quad dx_1/dt &= j_3(x_2x_3 - x_1) \\
[I^-]_{ss} \quad dx_2/dt &= -j_1x_2 + (j_1 + j_5)x_3x_4 - \\
&\quad (j_1 + j_5)x_2x_4 - j_3(x_2x_3 - x_1) + j_4x_3 \\
[IOH]_{ss} \quad dx_3/dt &= j_1x_2 - (j_1 + j_5)x_3x_4 + 2j_2(x_5 - x_3^2) - \\
&\quad j_3(x_2x_3 - x_1) - j_4x_3 + (j_4 + j_5)x_5 \\
[IO_2H]_{ss} \quad dx_4/dt &= j_1x_2 - (j_1 + j_5)x_3x_4 - \\
&\quad (j_4 + j_5)x_2x_4 + (j_4 + j_5)x_5 + j_5 \\
[I_2O]_{ss} \quad dx_5/dt &= (j_4 + j_5)x_2x_4 - j_2(x_5 - x_3^2) - (j_4 + j_5)x_5
\end{aligned}$$

The matrix of currents $\mathbf{V}(\mathbf{j})$ is defined as

$$\mathbf{V}(\mathbf{j}) = -\mathbf{S}(\text{diag } E_j)K^T$$

where K^T is the transpose of the matrix of the order of reactions K . Since $r_{ss} = E_j$, $\text{diag } E_j$ is a diagonal matrix whose elements are the reaction rates at the steady states. The stability depends on the sign of the real part of the eigenvalues of the matrix $\mathbf{M} = -(\text{diag } h) \mathbf{V}(\mathbf{j})$ where $\text{diag } h$ is a diagonal matrix whose elements are the reciprocals steady state concentrations ($h_i = 1/[X_i]_{ss}$, X_i) I_2 , I^- , HIO , HIO_2 , I_2O). Although the stability analysis by this method is much simpler than by direct linearization of the kinetic equations, it becomes limited for real models by the number and size of the required polynomials and the following sufficient instability condition is used. If at least one negative term exists in a principal minor of $\mathbf{V}(\mathbf{j})$, the steady state is unstable for some values of the parameters.

2.3. Dimensionless Equations

The last expressions of the kinetic equations throw some light on classical concepts in chemical kinetics, quasi-steady state approximation, nullclines and slow manifold. They are closely related and their use rests on the relative magnitude of some concentrations. The variables are already dimensionless and, since the number of dimensionless parameters is always less than classical ones, it is useful to define dimensionless parameters and dimensionless time based on a proper choice of the reference values:

$$\begin{aligned}
c_2 &= [I^-]_{ss}/[I_2]_{ss}, \quad c_3 = [IOH]_{ss}/[I_2]_{ss}, \\
c_4 &= [IO_2H]_{ss}/[I_2]_{ss}, \quad c_5 = [I_2O]_{ss}/[I]_{ss}, \quad \alpha = j_2/(j_4 + j_5), \\
\beta &= j_1/(j_4 + j_5), \quad \gamma = j_3/(j_4 + j_5), \quad \delta = j_5/(j_4 + j_5)
\end{aligned}$$

We take $[I_2]_{ss}$ as the reference concentration because it is larger than the concentrations of the other internal compounds $[I^-]_{ss}$, $[IOH]_{ss}$, $[IO_2H]_{ss}$, and $[I_2O]_{ss}$, such that c_2, c_3, c_4 and c_5 are small parameters. We take $(j_4 + j_5)$ as reference current rate because it is the rate of reaction (D) at the catalytic disproportionation steady state. We will see that this choice simplifies the relations between the dimensionless parameters and the properties of the chemical system. The corresponding dimensionless time is $\tau =$

$t(j_4 + j_5)/[I_2]_{ss}$. Introducing these parameters, the previous equations of motion take the dimensionless form.

$$\begin{aligned}
dx_1/d\tau &= \gamma(x_2x_3 - x_1) \\
c_2 dx_2/d\tau &= -\beta(x_2x_3 - x_4) - \gamma(x_2x_3 - x_1) + \\
&\quad \delta x_3(x_4 - 1) - x_2x_4 + x_3 \\
c_3 dx_3/d\tau &= \beta(x_2x_3 - x_4) - \gamma(x_2x_3 - x_1) + \\
&\quad 2\alpha(x_5 - x_3^2) - \delta x_3(x_4 - 1) - x_3 + x_5 \\
c_4 dx_4/d\tau &= \beta(x_2 - x_3x_4) + \delta(1 - x_3x_4) - x_2x_4 + x_5 \\
c_5 dx_5/d\tau &= -\alpha(x_5 - x_3^2) + x_2x_4 - x_5
\end{aligned} \tag{5}$$

These equations are similar to the classical SNA equations and have all their advantages together with the ones coming from their dimensionless form resulting from Pi theorem. Relations between the dimensionless parameters and the kinetic constants are easily derived from eqs. The following study of the slow manifold and the sensitivity analysis show the advantages of these equations over the classical ones.

2.4. Slow Manifold and Time Evolutions

The iodine concentration is much larger than the concentrations of the other internal compounds and taking $[I_2]_{ss}$ as reference concentration in eqs 5 simplifies greatly the study of the motion. The last four equations have the form $dx_i/dt = f_i(x, c)$ so that the trajectories in the state space are strongly attracted by the nullclines $f_i(x, c) = 0$. The equations of the four nullclines define the slow manifold. It is one dimensional in the five-dimensional state space. This is a first advantage of eqs 5 over the classical ones: they give directly simple equations of the slow manifold and show that the main effect of the parameters c_2, c_3, c_4 , and c_5 is to determine its attracting power. The equations (eqs 5) simplify also greatly the study of the shape of the slow manifold. They reveal that this shape depends only on the four parameters α, β, γ , and δ and not on the individual values of the ten rate constants.

At this point, we would like to underline the relation between the concepts of nullclines or slow manifold and the classical quasi-steady state approximation. The equations of the nullclines are identical to the equations we would write using the quasisteady state approximation but their meaning is clearer and this approach reveal a frequent misunderstanding in chemical kinetics. Taking for example the concentration $[I^-]$, the steadystate approximation does not mean that $d[I^-]/dt$ is equal to zero, what is clearly untrue. The slow manifold approach gives the exact condition: c_2 is small. Figure 1 shows examples of time evolutions calculated by numerical integration of eqs 5 and of slow manifolds calculated analytically when the disproportionation steady state is stable or unstable. The instability condition

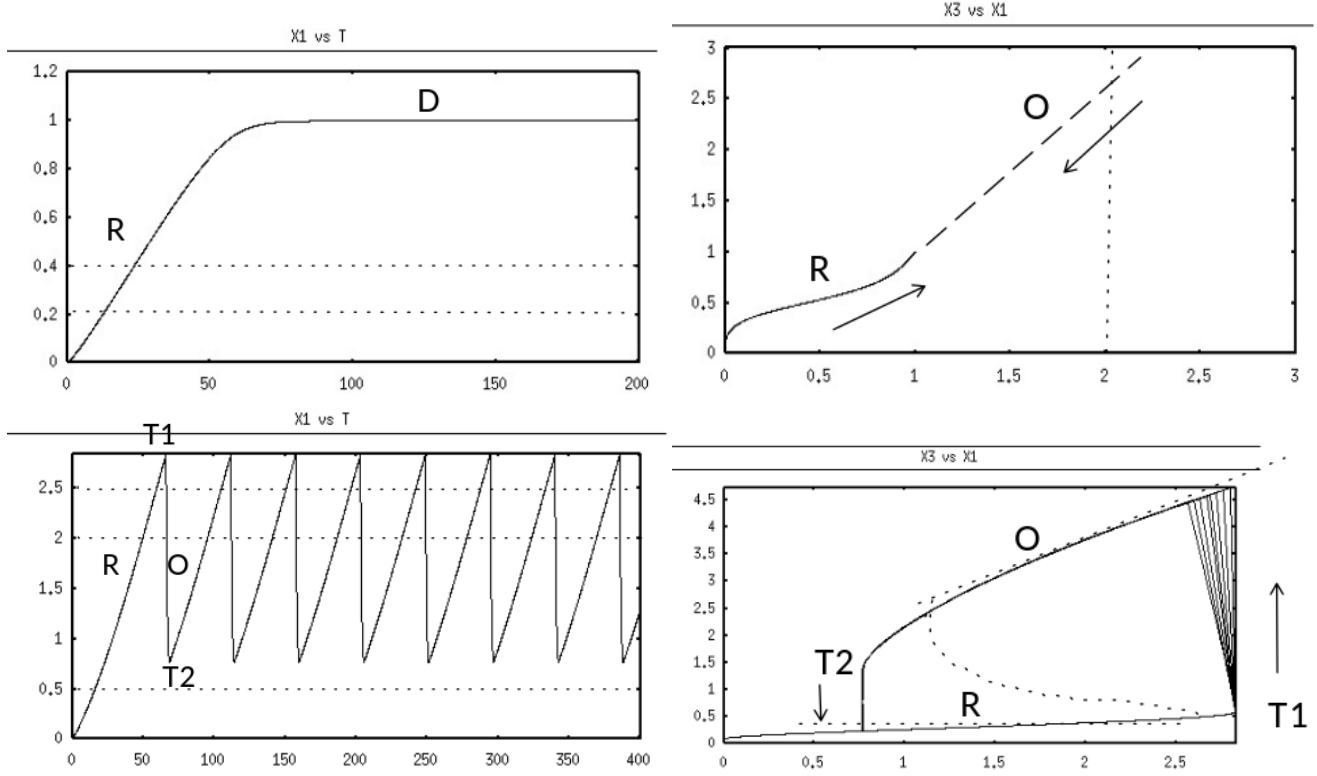


Figure 1. (a, b) Time evolution for $\alpha = 0.2$, $\beta = 0.01$, $\gamma = 100$, $\delta = 0.05$, $c_2 = 2 \times 10^{-4}$, $c_3 = 5 \times 10^{-4}$, $c_4 = 2 \times 10^{-4}$ and $c_5 = 2 \times 10^{-6}$ and projections of the trajectory (-) and the slow manifold (...) onto the $x_3 - x_1$ plane. The disproportionation steady state (b) is stable. (c, d) Same as parts a and b, except $\alpha = 2$. The disproportionation steady state (b) is unstable.

(eq 6) is obtained replacing the j_i in eq 4 with the dimensionless parameters. The simplification is striking.

$$(4\beta - \beta\delta + 3\delta - \delta^2)/\alpha + (11.5 - \beta)\beta < \delta^2 - 8\delta + 1 \quad (6)$$

The parameter α , equal to k_{+3}/k_6 , is the main parameter controlling the stability. The orders of magnitude of the other parameters are dictated by experimentally known orders of magnitude. The equilibrium of reaction (R4) being only weakly disturbed during the Bray-Liebhafsky reaction, its exchange current rate j_3 is much larger than the sum of current rates $j_4 + j_5$. The value of $\gamma = j_3/(j_4 + j_5)$ must be much larger than one and has a minor influence on the shape of the calculated curves. The current rate j_3 does not appear in eq 4 and the parameter γ does not appear in eq 6 for the same reason. On the contrary, the equilibrium of reaction (R1) is strongly disturbed, its exchange current rate j_1 must be relatively small and $\beta = j_1/(j_4 + j_5)$ must be small. The parameter δ , equal to $j_5/(j_4 + j_5)$, is the relative contribution of reaction (R8) to reaction D. The values of c_2 and c_3 used in Figure 1 are based on experimentally known orders of magnitude of the concentrations while the values of c_4 and c_5 are unknown. However, as explained before, their values have nearly no influence on the calculated curves as

long as they remain small. Parts a and b of Figure 1 illustrate the motion when the disproportionation steady state is stable. As expected, the trajectories calculated numerically are close to the slow manifold calculated analytically. The evolution begins with reaction R because the initial value of x_1 (iodine) is zero. When the initial value of x_1 is larger than one, the evolution begins with reaction O. Parts c and d of Figure 1 illustrate the motion when the disproportionation steady state is unstable. The x_1 oscillations obtained by numerical integration of the eqs 5 are very similar to the experimental ones. The oscillations can be divided into two periods separated by transition points. During the period R the rate of reaction R is larger than the rate of reaction O and x_1 increases; during the period O, it is the opposite and x_1 decreases.

Figure 1d shows the projections of the slow manifold and of the trajectory from the five dimensional state space onto the $x_3 - x_1$ plane explaining the transition points T1 and T2. The slow manifold has an S shape with upper and lower stable branches and an intermediate unstable branch between points T1 and T2. The calculated trajectory follows the lower branch until it reaches point T1. At this point, dx_1/dt is still positive and the trajectory must leave the slow manifold. It jumps quickly (more or less quickly depending on

the smallness of the ci) to the stable upper branch where dx_1/dt is negative and follows this branch to point T2. Then it must again leave the slow manifold, jumps to its lower branch and closes the limit cycle.

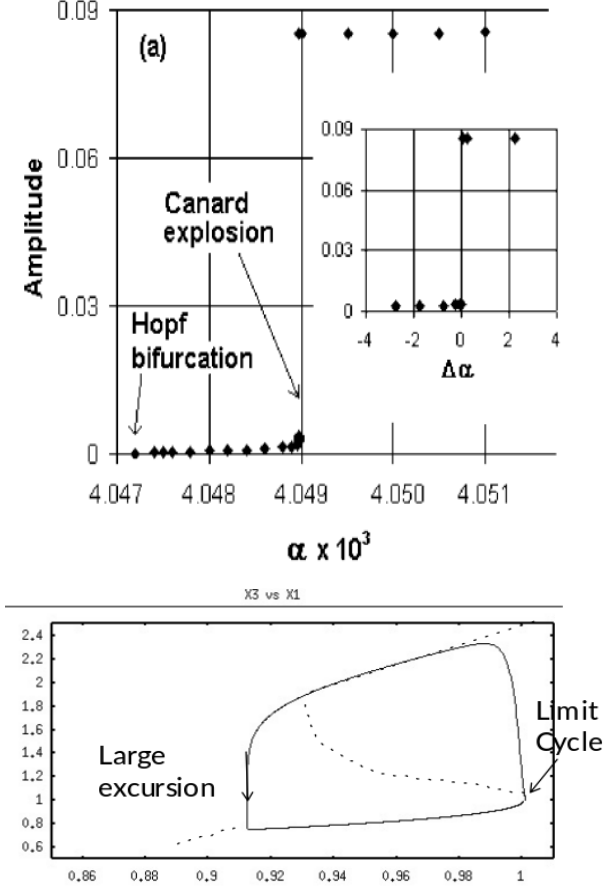


Figure2

2.5. The Bifurcation Points

We have studied the transitions between stability and instability using $\alpha = j_2/(j_4 + j_5) = k_{+3}/k_6$ as bifurcation parameter. When the steady state is stable and is far from a bifurcation, the slow manifold has a shape like in Fig 1b leading to the smooth disproportionation. When the disproportionation steady state is unstable, the slow manifold has an S shape as in Fig 1d leading to oscillations. Between these two situations surprising behaviours are observed. At the transitions between stability and instability, the slow manifold has still an S shape and the steady state is close to one of the points T1 or T2. The first case is favored by low δ values and will be illustrated by the example in Fig 2. The second case is favored by high δ values and will be illustrated by the example in Fig 3. The parameter δ has always a stabilizing effect and the meaning of “high δ values” is defined by the instability condition 6. As $\delta = j_5/(j_4 + j_5) < 1$, its left-hand side is positive and the instability condition

6 cannot be satisfied if its right-hand side is negative, that is, if $\delta^2 - 8\delta + 1 < 0$ or $\delta > 0.127$. The parameter β has also a stabilizing effect and the amplitude of the studied phenomena increases when β decreases because the left-hand side term decreases. The other parameters were chosen as explained before.

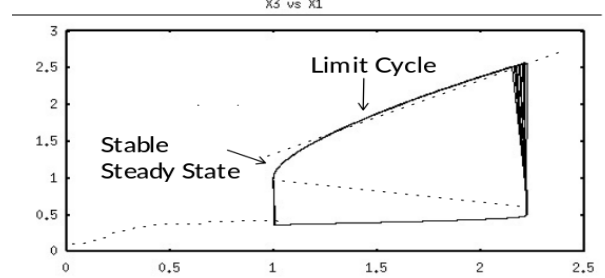
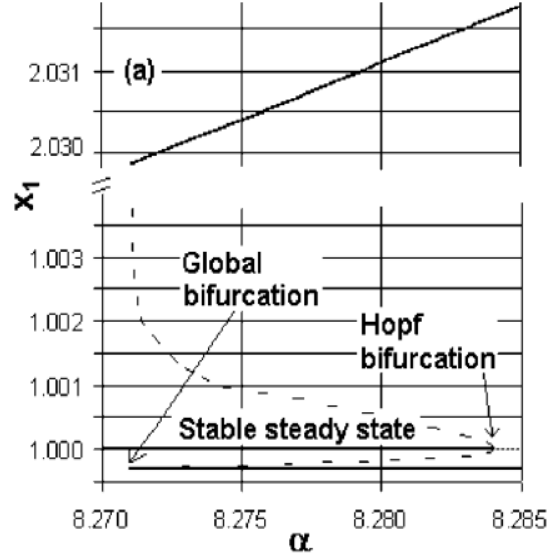


Figure3

Figure 2 gives an example of bifurcation when the steady state is close to T1. A supercritical Hopf bifurcation is found by numerical simulations for $\alpha = 4.0473 \times 10^{-3}$, very close to $\alpha = 4.0465 \times 10^{-3}$ given by condition 6. The small difference comes from the numerous small terms neglected in the characteristic equation. When α increases over $\alpha = 4.0473 \times 10^{-3}$ the limit cycle born at the Hopf bifurcation grows and a situation similar to that in Figure 1d is finally obtained. However, this growth can be more or less fast depending on the values of the other parameters. Figure 2a gives an example of abrupt increase of the oscillations amplitude near $\alpha_c = 4.04897475 \times 10^{-3}$, known as a canard explosion. This phenomenon is characteristic of systems with very different time scales, which is our case, and can be continuous or not. The insert in Figure 2a suggests that it is discontinuous for the used values of the param-

ters. Such canard explosions are often associated with excitability, and Figure 2b shows the behavior for $\alpha = 4.0489 \times 10^{-3}$, just before the explosion. The unstable steady state is surrounded by a very small limit cycle and the system is highly excitable because the trajectory is strongly attracted by the slow manifold. For the chosen initial values, the system makes a large excursion near the slow manifold before cycling toward the small limit cycle. This excursion announces the large limit cycle that will appear at the canard point.

Figure 3 shows an example of bifurcation when the steady state is close to T2. When α increases from 8.2710 to 8.2711, a large limit cycle seems to appear from nowhere and to understand what happens it is easier to consider decreasing values. For high αR values the disproportionation steady state is unstable and surrounded by a limit cycle. Near $\alpha = 8.284$ a subcritical Hopf bifurcation is observed. The steady state becomes stable but is still surrounded by a limit cycle. For $\alpha < 8.284$ bistability is observed as in Figure 3b. They are two basins of attraction, one for the steady state, the other for the limit cycle. They are separated in the five-dimensional state space by a four-dimensional manifold called the separatrix. Figure 3a shows a section in it. When α continue to decrease a new bifurcation is encountered: the separatrix collides with the limit cycle near $\alpha = 8.2711$ and breaks it. The large limit cycle disappears suddenly. For lower α values the only attractor is the stable steady state but the system can perform large excursions near the former limit cycle before reaching it. Let us note that the difference between the α values at the two bifurcations is so small that they could probably not be resolved experimentally. Only a sudden transition between a stable steady state and a limit cycle with a finite size would be observed. Our example shows that this sudden transition would be an illusion and that normal transitions lay under it.

3. References

Stoichiometric network analysis

Bifurcation analysis of the reduced model of the Bray–Liebhafsky reaction

Mechanism of the Bray–Liebhafsky reaction: effect of the oxidation of iodous acid by hydrogen peroxide

Investigation of Dynamic Behavior of the BrayLiebhafsky Reaction in the CSTR. Determination of Bifurcation Points

Stoichiometric Network Analysis and Associated Dimensionless Kinetic Equations. Application to a Model of the BrayLiebhafsky Reaction

Stoichiometric network analysis and associated dimensionless kinetic equations. Application to a model of the Bray–Liebhafsky reaction